Single-Epoch Ambiguity Resolution for kinematic GNSS Positioning

Christian Eling, Philipp Zeimetz, Heiner Kuhlmann
Institute of Geodesy and Geoinformation, University of Bonn, Germany

Abstract
Automatic machine control requires accurate and reliable information about the latest attitude and position of the vehicle. In addition to inertial sensors and odometer Global Navigation Satellite Systems (GNSS) are well established in the determination of these parameters.
Besides code observations GNSS additionally provide carrier-phase measurements, which should be used to achieve high accuracies. Certainly, the key to GNSS carrier-phase positioning is the ambiguity resolution. This is the process resolving the unknown number of integer cycles in the carrier phase data. Principally, different approaches exist to resolve the ambiguities. Since multi-epoch techniques lead to a substantial loss of possible solutions, a single-epoch ambiguity resolution should be aimed at.
A common procedure that enables an ambiguity resolution for every single epoch is the Ambiguity Function Method (AFM). By means of a cost function the AFM tests candidates corresponding to a generated search space, including possible rover positions. However, by use of this approach disadvantages occur due to the computation time, increasing with the size of the search space, and the reliability, depending on the decidedness of the complicated multipeak-function. Accordingly, the candidates in the search space have to be selected carefully. For this purpose, position approximations can be achieved by use of GNSS-velocities, a vehicle motion model, differential code-solutions as well as Kalman filtering. Therefore, through the combination of these tools it was possible to develop a single-epoch ambiguity resolution algorithm that also shows good performances in urban areas with a success rate of 96.59 %.

Keywords
GNSS, ambiguity resolution, Kalman filtering, GNSS velocities

1 INTRODUCTION

In the field of automated control as well as supported navigation of machines Global Navigation Satellite Systems (GNSS) are of major importance, since they allow for the determination of absolute positions, attitudes and velocities. On this account most of the land- and construction-machines are nowadays already equipped with at least one GNSS antenna. Besides pseudoranges GNSS also provide more precise carrier phase measurements. Within differential positioning based on double differenced carrier phases, sub-centimetre-level precision GNSS positioning becomes possible. However, it is well known that GNSS double differenced carrier phase measurements are ambiguous by an unknown number of integer cycles. To fully exploit the high accuracy of the carrier phase observables, the ambiguities must be resolved to their correct integer value (Hoffmann-Wellenhof et al., 2008). Especially in urban areas obstacles like street canyons, bridges or vegetation lead to frequent losses of lock, which always necessitate a new ambiguity resolution. Therefore, for kinematic applications, the duration of the ambiguity resolution is of particular importance.
In this contribution we will first give a short overview of the existing ambiguity resolution techniques. Afterwards we will present a single-epoch ambiguity resolution method for kinematic positioning, which is based on the combination of approaches like GNSS velocity determination and Kalman filtering with an instantaneous ambiguity resolution technique. By means of test runs, the procedure was tested successfully.

2 AMBIGUITY RESOLUTION BACKGROUND

In the last decades integer ambiguity resolution was the focus of many researchers, since the ambiguity resolution is the key to precise GNSS positioning. Therefore, many different techniques exist to determine the unknown integer cycles of the observed double differences. Generally, these approaches can be classified into three categories: ambiguity resolution in the measurement domain, search technique in the ambiguity domain and search technique in the coordinate domain (Kim and Langley, 2000).

The ambiguity resolution in the measurement domain is principally based on code observations. Since code observations are more inexact than carrier phase measurements, these approaches are ordinarily not very suitable. Only the processing of interfrequency linear combinations enables a more or less reliable ambiguity resolution. However, this requires the observation of at least 2 frequencies.

The second class of ambiguity resolution techniques contains approaches searching in the ambiguity domain. Generally, they are based on the so called integer least squares (ILS) theory (Teunissen, 1993). The ILS-approaches consist of three steps. By means of a float solution the cycles are estimated via a least squares adjustment. Using the resulting float ambiguities and the variance-covariance matrix the odd number of ambiguities can afterwards be fixed within a search process in the integer ambiguity estimation step. As soon as the ambiguities are set to integer values a fixed solution follows to determine the precise baseline parameters. The most famous and reliable ILS ambiguity resolution technique is the LAMBDA method (e.g. Teunissen, 1995). Further well known approaches are the FASF (Chen and Lachapelle, 1995), the FARA (Frei and Beutler, 1990), the OMEGA (Kim and Langley, 1999) and the LSAST (Hatch, 1990) method. Except the LSAST method, all of these search techniques are multi-epoch approaches. This is because the float solution step necessitates the usage of observations from more than one epoch, since the number of parameters definitely exceeds the number of available double differences in one single epoch.

The third class of ambiguity resolution techniques contains approaches searching in the coordinate domain. The most famous of these methods and simultaneously one of the earliest ambiguity resolution search techniques in general is the Ambiguity Function Method (AFM) (Counselman and Gourevitch, 1981; Remondi, 1984; Mader, 1990). On the basis of appropriate criteria, candidates of a predefined search space have to be tested, only regarding the fractional part of the observed carrier phases of one single epoch. In this paper, this method is the basis for further investigations.

3 INSTANTANEOUS AMBIGUITY RESOLUTION

In case of kinematic applications the rapidity of the ambiguity resolution is of particular importance. Therefore, fixing the integer number of cycles of the observed double differences within one single epoch should be aimed at. Moreover, not only long term signal interruptions appear very often during kinematic applications. Even cycle slips and interruptions to the signal between epochs occur, which result in new sets of integers (Corbett and Cross, 1995). To avoid additional processing during cycle slip detection a single epoch ambiguity resolution is inevitable.

Since the AFM is not in need of float ambiguities or a variance-covariance matrix it is well-suited for instantaneous ambiguity resolution and therefore also resistant to cycle slips. For these reasons, we now like to introduce the basic principle of the AFM.

As mentioned above, the ambiguity search using the AFM takes place in the coordinate domain. Maximizing the Ambiguity Resolution Function (ARF) enables the assessment of candidates of a predefined search space, containing possible rover positions.

The ARF, for the single frequency case, can be written as (Lachapelle et al., 1992):

$$ARF\left(X_C, Y_C, Z_C\right) = \sum_{m=1}^{N-1} \cos 2\pi \left(\nabla\Delta\phi_{obs}^{kj}[E1 \mid E2] - \nabla\Delta\phi_{calc}^{kj}[E1 \mid X_C, Y_C, Z_C]\right) \tag{1}$$

whereas $\nabla\Delta\phi^{kj}{}_{obs}$ is the observed and $\nabla\Delta\phi^{kj}{}_{calc}$ a calculated double difference of the satellites *k* and *j*. Since *E1* is the known position of the master antenna, the ARF is only dependent on the coordinates of the candidates, which are located in the search space around the true rover position *E2* (see figure 1). In case the position of the candidate (X_C, Y_C, Z_C) is similar to *E2*, the difference between the observed and the calculated double difference corresponds to the unknown ambiguities in order that the result of the cost function is equal to 1. Considering the carrier phase measurements of *N* satellites on *w* frequencies the outcome of the ARF would ideally be *(N-1)·w*, taking into account that due to multipath and receiver noise this maximum will never be reached.

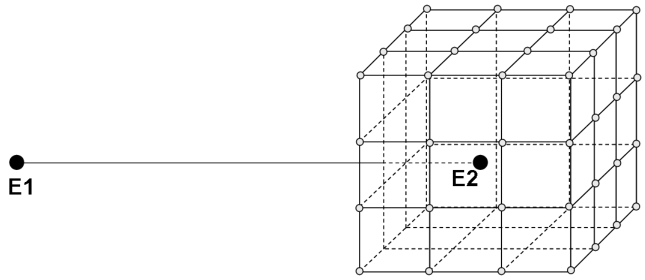

Figure 1: Depiction of a possible search space for the AFM.

However, there are two drawbacks of the AFM. First, the computational efficiency is highly dependent on the size of the search space, which is defined by the accuracy of the approximate position. Therefore, the computation time can potentially be very long. And second there may be several maxima points that the AFM must discriminate between to find the optimal solution (Han and Rizos, 1995). Consequently, the basic AFM approach has to be improved to make it suitable for practice.

4 EFFICIENCY IMPROVEMENT OF THE AFM

The key to reliable and fast ambiguity fixing by means of the AFM is a reduction of the size of the search space. In so doing, the computation time decreases heavily. Furthermore, false candidates can be excluded with the result that the decision-making of the AFM will be simplified.
In the creation of the search space two cases can be decided. On the one hand the first time initialization or re-initialization after a GNSS gap and on the other hand the transfer between two epochs as long as GNSS is available.

4.1 First-time initialization or re-initialization of the ambiguities

In the beginning of an application as well as in consequence of a gap of the GNSS signals, a first-time initialization or a re-initialization of the ambiguities is necessary. The starting point for this search process is an approximate rover position to generate a search volume. Without the use of additional sensors, there are only few opportunities for determining these preliminary coordinates. In most cases code observations are preferably used to cope with this task. By means of differenced code signals accuracies in the range of a few decimetres to metres are achievable. Linear combinations such as the wide lane also enable the determination of an approximate position (Abidin, 1994). However, this requires the observation of at least two frequencies, which is not always given, e.g. low-cost receivers. Therefore, we use differential code-observations for the determination of an approximate rover position in case of first-time or re-initialization of the ambiguities. Even if the ambiguities could be fixed correctly in the first epoch after a loss of lock, this initialization process will be delayed for more than one epoch to avoid an incorrect first-time or re-initialization. During this time the preliminary coordinates are filtered in an Extended Kalman Filter (EKF) to improve the reliability of the ambiguity resolution (see chapt.5).
In order to consider the balance between the computational effort of the search process and the size of the search space, which has to be large enough to contain the true rover position, the configuration of the candidates should be carefully selected. Since the candidates vary on the basis of different ambiguities, the possible rover positions in the search space are also dependent on different sets of integer ambiguities. Therefore, the approximate rover position is used to determine the ambiguities of the observed double differences, which can be rounded to integer cycles. Afterwards these ambiguities need to be varied for different values to determine possible rover positions. In order to limit the number of candidates in the search space, not all double difference ambiguities, but only three should be used for generating the search space. The selection of this three primary observations occurs in consideration of the position dilution of precision (PDOP), the elevation angles as well as residuals of the code solution. In case the range of the ambiguities is set from minus five to plus five values the

search volume consists of 1331 ($[(2*5)+1]^3$) sets of ambiguities, which lead to possible positions, including the true rover position (Corbett and Cross, 1995). Depending on the PDOP, the edges of the cubic search space reach lengths up to 10 m. Therefore, the search space is first defined in the ambiguity domain before it is used to generate a physical space, defined in the coordinate domain. Finally, the ambiguity resolution of all double differences occurs by testing the candidates by means of the AFM. Since the ARF is a multi peak function the results are not inevitably unambiguous (see chapt.4.3). In case the maximum of the ARF cannot be clearly distinguished from side-lobes, further investigations are necessary to find the correct set of ambiguities. Criteria are for example the variances of a least squares adjustment in the determination of the baseline parameters.

4.2 Position update using GNSS-velocities

Once the ambiguities were fixed and at least four GNSS satellites are visible in two successive epochs, the determination of an approximate rover position can occur by use of integrated GNSS-velocities in combination with a Kalman filter. This is because the GNSS-velocities are also based on precise carrier phase measurements, whereas they are not in need of an ambiguity resolution. This becomes obvious regarding the observations used for the velocity determination, consisting of the first order difference approximation of the carrier-phase observations (Serrano et al., 2004):

$$\dot{\phi}_i^j \approx \frac{\phi_i^j - \phi_{i-\Delta t}^j}{\Delta t} \qquad (2)$$

where ϕ is the fractional carrier-phase of the satellite j, i is the observation epoch and Δt the sampling rate. The velocity determination occurs by use of a least squares adjustment based on the following objective function:

$$\dot{\phi}_i^j = \boldsymbol{h}_i^j \cdot \left(\boldsymbol{v}_i^j - \boldsymbol{V}_i\right) + \dot{B}_i + \varepsilon_i^j \qquad (3)$$

Where $\boldsymbol{V}$ is a vector containing the unknown receiver velocities (V_x, V_y and V_z). $\boldsymbol{v}$ represents the satellite velocity vector, which can be computed by use of the ephemeris. $\boldsymbol{h}$ stands for the directional cosine between the receiver and the satellite:

$$\boldsymbol{h}_i^{jT} = \frac{\left(\boldsymbol{S}_i^j - \boldsymbol{X}_i\right)}{|\, \boldsymbol{S}_i^j - \boldsymbol{X}_i \,|} \qquad (4)$$

whereas $\boldsymbol{S}$ is the position vector of satellite j and $\boldsymbol{X}$ the receiver position vector. Furthermore, $\dot{B}$ are the receiver clock drift and ε the receiver noise.
By means of equations (2)-(4) the receiver velocity can be determined in every observation epoch i. Of course the resulting velocities are not the true ones for the actual epoch, since the first order difference approximation in equation (2) enables the estimation of the mean velocity between the epochs i and i-Δt, but in case of sampling rates higher than 1 Hz, they are still accurate enough to deliver a suitable approximate position for the AFM.

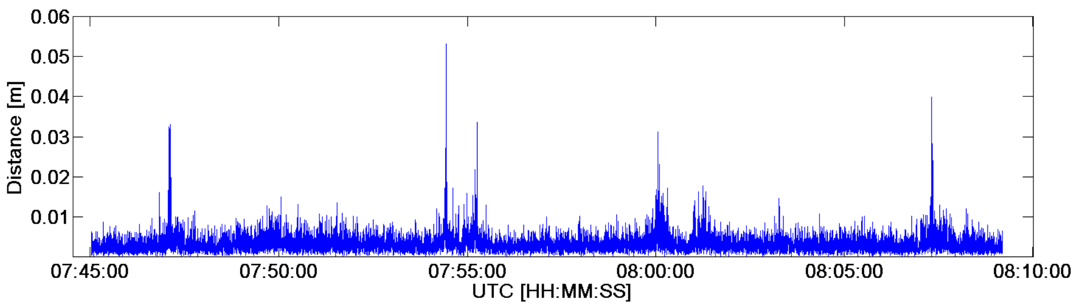

Figure 2: Distances between integrated GNSS velocity positions and final positions.

To underline this, the distances between the approximate positions, calculated by integration of the velocities, and the final positions during a kinematic experiment are presented in figure 2. Except for a few outliers, the total deviations are mostly less than 1 cm. The mean of the distances between the approximate and the final positions is about 3 mm. The clearly visible outliers are based on poor GNSS measurement conditions. However, these deviations are less than 6 cm whereas the wavelengths of GNSS signals are in the order of 20 cm. According to this, the filtered approximate positions are still well suited to reduce the size of the search space. Therefore, as long as GNSS is available the GNSS velocities are used to define the search volume.

4.3 Reducing the number of maxima in the AFM

One drawback of single-epoch ambiguity resolution approaches is the susceptibility in case of poor GNSS measurement conditions. Biases like multipath, residual atmospheric effects and satellite orbit errors lead to deviations in the observed carrier phases (Kim and Langley, 2000). Therefore, it cannot be excluded that false ambiguities will be selected from the set of candidates in the search space, since the multi peak ARF does not allow for an unambiguous decision in such epochs. To improve the performance of single-epoch ambiguity resolution techniques approaches employing linear filters for the residuals or time averages for the objective function showed good performances in earlier studies (e.g. Borge and Forssell, 1994; Martin-Neira et al., 1995). Therefore, the decision-making of the AFM should also be improvable.

In our single-epoch ambiguity resolution approach we use a Kalman filter to predict the residuals of the observed double differences in every epoch. Since the residuals cannot be described by any motion behaviour a random-walk-process is applied as motion model in this procedure. Accordingly, the discrete system equation follows:

$$\begin{vmatrix} x_R(k+1) \\ \Delta x_R(k+1) \end{vmatrix} = \begin{vmatrix} 1 & \Delta t \\ 0 & 1 \end{vmatrix} \cdot \begin{vmatrix} x_R(k) \\ \Delta x_R(k) \end{vmatrix} + \begin{vmatrix} \Delta t \\ 1 \end{vmatrix} \cdot w(k) \tag{5}$$

$$\boldsymbol{x}(k+1) = \boldsymbol{T}(k) \cdot \boldsymbol{x}(k) + \boldsymbol{S}(k) \cdot w(k) \tag{6}$$

whereas $\boldsymbol{x}(k)$ is the state vector, containing the filtered residual x_R and the derivative of the residual Δx_R. $\boldsymbol{T}$(k) is the transition matrix, $\boldsymbol{S}$(k) the system noise coupling and w(k) the system noise. By use of this Kalman filter the residuals of every observed double-difference can be predicted from epoch *i-1* to epoch *i*. Therefore, the performance of the ambiguity resolution can be improved by reducing the deviations of the observations in the AFM using the predicted residuals.

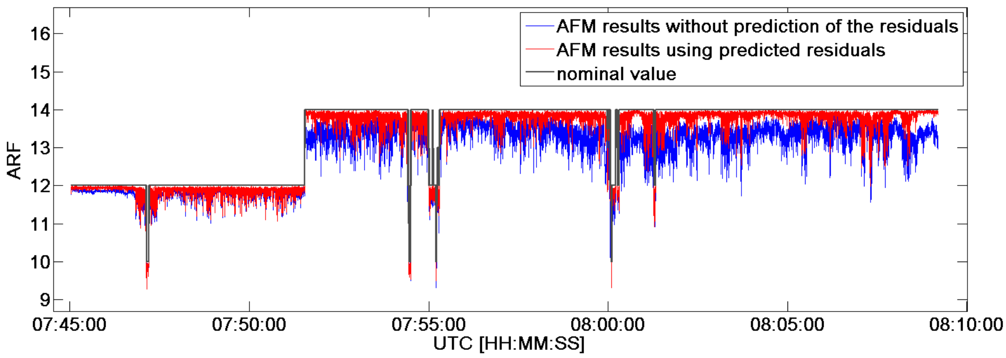

Figure 3: Comparison of results of the ARF using and disregarding the prediction of the residuals.

In figure 3 a comparison of the outcome of the AFM disregarding and using the residuals prediction during a kinematic test is presented. According to this, the maxima of the ARF increase by use of the Kalman filter, with the result that they obviously come closer to the nominal value of $(N\text{-}1)\cdot w$. However, this does not imply a simplification in the discrimination of false and correct solutions in the search space, since a simultaneously increase of the side-lobes is also possible. In order to demonstrate the actual impact of the filter process, the outcome of the ARF for every candidate of the search space during one epoch is presented for two cases, using and disregarding the filtered residuals, in figure 4. Therefore, not only the size of the maxima but also the difference to side-lobes increases by use of the prediction step. Summarizing this section, there are two reasons why the single-epoch ambiguity resolution has become better. On the one hand, the maximum of the outcome increases. And furthermore, the correct solution is now in greater contrast to incorrect sets of ambiguities. Therefore, there are no more investigations necessary to come to a decision, which candidate of the search space leads to the best and correct ambiguities.

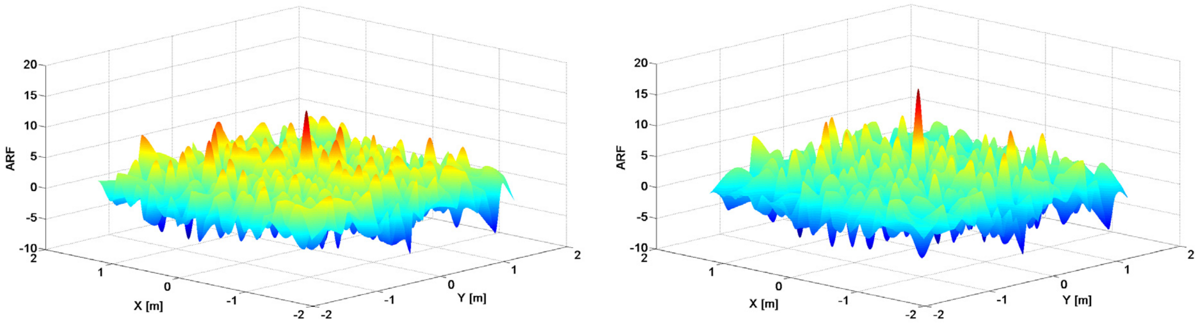

Figure 4: Results of the ARF disregarding (left) and using (right) the residuals prediction for one epoch.

5 EXTENDED KALMAN FILTER

As mentioned above, an EKF is used to improve the reliability of the determined rover positions in this system. Generally, an EKF is a recursive algorithm that enables the combination of noisy measurements with a priori known motion behaviour of a vehicle, to estimate an optimal state vector as time progress on the basis of external observations, (e.g. Grewel et al., 2007). Depending on the correctness of the used motion model the EKF is well suited to reduce white noise and to detect outliers. Since vehicles mostly move on streets, which are compiled of the basic elements straight, arc and clothoide, we assume a uniform circle movement as system dynamics model (Aussems, 1999; Eichhorn, 2005):

$$\bar{\boldsymbol{x}}_{k+1} = \begin{bmatrix} \begin{vmatrix} \hat{x}_k^G \\ \hat{y}_k^G \\ \hat{z}_k^G \end{vmatrix} + R_L^G \begin{vmatrix} \Delta East_k \\ \Delta North_k \\ \Delta Up_k \end{vmatrix} \\ \hat{\alpha}_k + \Delta\hat{\alpha}_k \\ \hat{v}_k \\ \Delta\hat{\alpha}_k \\ \Delta\hat{h}_k \end{bmatrix} \qquad \begin{aligned} \Delta East_k &= \frac{-\Delta t \cdot \hat{v}_k \cdot \left(\cos(\hat{\alpha}_k + \Delta\hat{\alpha}_k) - \cos(\hat{\alpha}_k)\right)}{\Delta\hat{\alpha}_k} \\ \Delta North_k &= \frac{\Delta t \cdot \hat{v}_k \cdot \left(\sin(\hat{\alpha}_k + \Delta\hat{\alpha}_k) - \sin(\hat{\alpha}_k)\right)}{\Delta\hat{\alpha}_k} \\ \Delta Up_k &= \Delta\hat{h}_k \end{aligned} \tag{7}$$

whereas x,y,z are the cartesian coordinates from the epoch k, α is the heading, $\Delta\alpha$ the heading change, v is the velocity in driving direction and Δh is the altitude change. R_L^G represents the rotation matrix to transform the coordinate changes $\Delta East$, $\Delta North$ and ΔUp from the local level frame to the global geocentric coordinate frame (Hoffmann-Wellenhof et al., 2008):

$$R_L^G = \begin{vmatrix} -\sin\lambda & -\sin\varphi\cos\lambda & \cos\varphi\cos\lambda \\ \cos\lambda & -\sin\varphi\sin\lambda & \cos\varphi\sin\lambda \\ 0 & \cos\varphi & \sin\varphi \end{vmatrix}. \tag{8}$$

Thereby λ stands for the longitude and φ for the latitude.
According to this, the transition matrix $\boldsymbol{T}$ consists of the derivatives of equation (7) with respect to the states $\boldsymbol{x} = |x^G\ y^G\ z^G\ \alpha\ v\ \Delta\alpha\ \Delta h|^T$. The system noise coupling $\boldsymbol{S}$ contains the derivatives of equation (7) with respect to v, $\Delta\alpha$ and Δh, integrated over the sampling rate Δt, with the result that the discrete system equation (6) allows for accelerations, updates of the heading changes as well as updates of the altitude changes. The measurement equation (9) establishes the connection between the state vector $\boldsymbol{x}$ and the observations, given by the design matrix $\boldsymbol{H}$ and a white noise ε. The observation vector $\boldsymbol{l}=|x^{GPS},y^{GPS},z^{GPS},v^{GPS}|^T$ consists of the GPS rover position and the rover velocity. This rover velocity is the norm of the East and North component of the transformed GPS rover velocity vector $\boldsymbol{V}$, which can be estimated by means of eq. (3). $\boldsymbol{D}$ is a unit vector $\boldsymbol{D} = |1\ 0\ 0|$.

$$\begin{vmatrix} x_{k+1}^{GPS} & y_{k+1}^{GPS} & z_{k+1}^{GPS} & v_{k+1}^{GPS} \end{vmatrix}^T = \begin{vmatrix} I_{3x3} & 0_{3x4} \\ 0_{1x4} & D \end{vmatrix} \cdot \begin{vmatrix} \bar{x}_{k+1}^G & \bar{y}_{k+1}^G & \bar{z}_{k+1}^G & \bar{\alpha}_{k+1} & \bar{v}_{k+1} & \Delta\bar{\alpha}_{k+1} & \Delta\bar{h}_{k+1} \end{vmatrix}^T + \varepsilon \tag{9}$$

Outliers, which are attributable to multipath or incorrect fixed ambiguities, can be detected by an innovation test. Besides the reduction of white noise as well as the detection of outliers, the system dynamics model of the EKF also allows for bridging GNSS gaps. In figure 5 two examples for this type of application are shown. In the left chart, the GNSS gap only lasts 25 epochs, with the result that the prediction is working very well. Therefore, in case of a short term GNSS outage, which can for example be caused by a tree, it is well suited to detect outliers, which are not uncommon during the first epochs after a signal interruption. However, in the right chart, a long term signal interruption is presented (146 epochs). In this case, the prediction does not completely agree with the true motion behaviour, in order that the EKF has to be restarted, once the ambiguities are fixed.

By adding further sensors, like gyroscopes or odometer, the bridging of long term GNSS gaps can also still be improved, in order that the deviations to the true position would only increase very slowly.

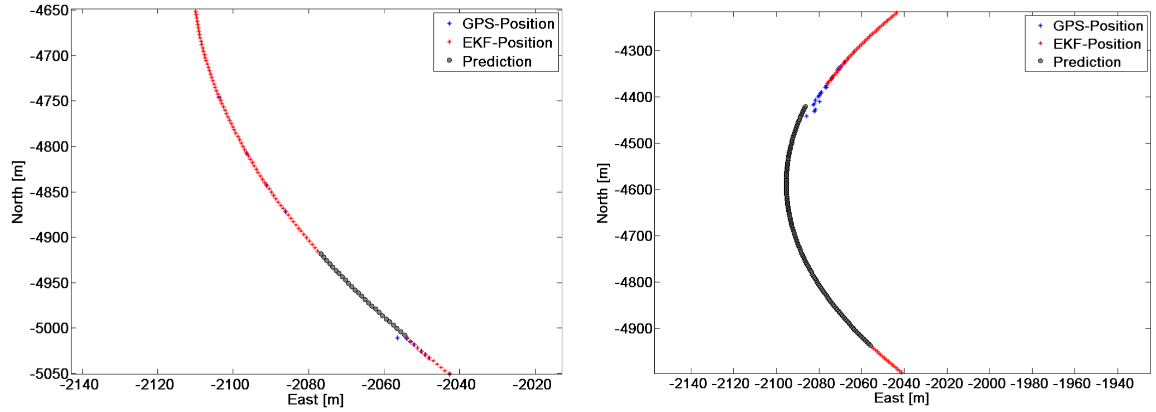

Figure 5: Prediction of the states during GNSS gaps by use of the system dynamics model.

The entire single epoch ambiguity resolution approach for the determination of GNSS positions during kinematic applications is presented in a flow chart in figure 6. Accordingly, the ambiguity resolution either occurs by use of a Kalman filtered code position or a position update based on GNSS velocities. In case no GNSS observations are available, the states are predicted by the system dynamics model presented in equation (7).

6 RESULTS

The developed single epoch ambiguity resolution approach for kinematic GNSS positioning was tested by means of different experiments. In order to identify the correctness of the ambiguity resolution, the results were compared to commercial software. The outcome of this commercial software of a test run, carried out on freeways and city avenues in and near Bonn, is presented in figure 6. Especially in urban areas this post processing led to less pleasant results, since most of the positions are based on imprecise code observations. The reason is that the commercial software could not fix the ambiguities quickly after each of the numerous signal interruptions. Therefore, this example emphasises the necessity of a single-epoch ambiguity resolution in case of kinematic applications, since a multi-epoch approach leads to long-term GNSS gaps after signal interruptions.

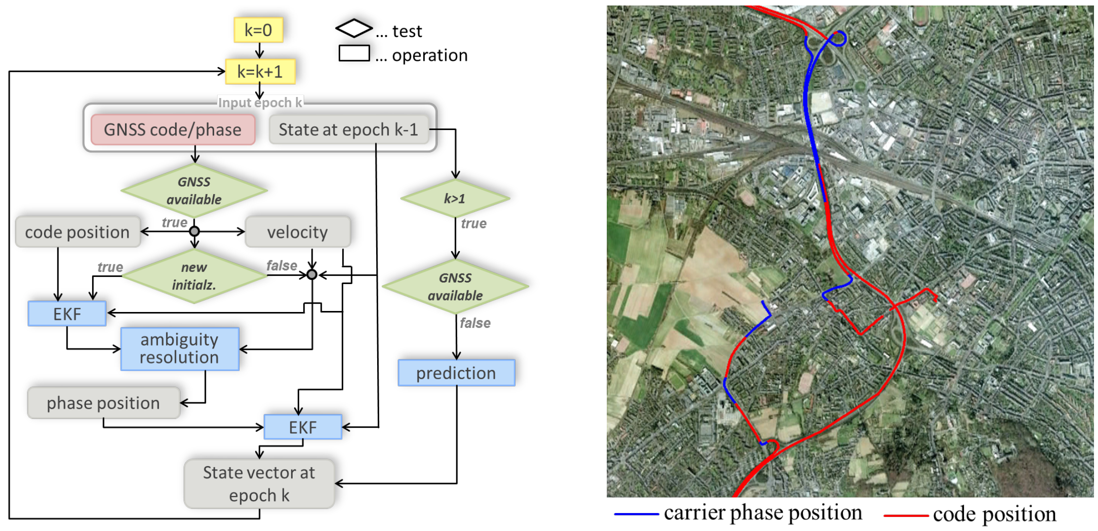

Figure 6: Flow chart of the developed approach (left) and test run processed by com. software (right)

The same dataset was also analyzed by means of the presented single-epoch approach. The sampling rate during this test run, in which speeds up to 140 km/h were reached, was 10 Hz. In table 1 the success rates of the ambiguity resolution for all of the 20294 epochs are shown. As expected, the reliability of the ambiguity resolution depends on the number of visible satellites. This is mainly because of the distinctness between correct and false sets of ambiguities in the AFM. The less observations are available the increased is the influence of multipath effects of individual signals. However, still 89.46% of the epochs, in times only four satellites were visible, led to correct ambiguity resolutions. In case more than six satellites were visible, the success rate increases 98 % whereas in 99.65% of all the epochs, where 9 satellites were visible, the ambiguities could be fixed correctly.

Table 1: Success rates of the ambiguity resolution by use of the single-epoch approach.

visible satellites	epochs	incorrect resolutions	success rate
4	2240	236	89.46 %
5	2320	183	91.98 %
6	3153	136	95.69 %
7	4492	85	98.11 %
8	4961	42	99.15 %
9	3128	11	99.65 %
sum	20294	693	96.59 %

Besides the success rates the time to fix the ambiguities is also of interest, since the objective of the single-epoch approach is to find the correct set of ambiguities as fast as possible after a signal interruption. In table 2 the number of epochs needed to find the true ambiguity resolution is presented for different re-initializations during the kinematic experiment. For comparison, the number of epochs elapsed until re-initialization is also shown for the outcome of the commercial software. In case of the single-epoch approach it should be noticed that not all of these epochs led to incorrect ambiguities, but rather the ambiguity resolutions were inconstant during these listed epochs.

Table 2: Comparison of epochs needed to re-initialize the ambiguities after GNSS gaps.

	epochs elapsed until re-initialization	
re-initialization	single-epoch approach	commercial software
1	2	52
2	3	324
3	27	85
4	2	37
5	3	51
6	3	58
7	2	58
8	37	20
9	12	50
10	10	403
11	20	47
12	14	85
13	7	38
14	5	206
15	2	57
16	10	73
17	2	278

According to this, the single epoch approach is mostly a lot faster than the commercial software. In many cases, it was possible to fix the ambiguities in the second epoch beyond a signal interruption. Especially in case of the second, the tenth, the fourteenth and seventeenth re-initialization the difference between both approaches is particularly evident, since the commercial software requires above two hundred epochs more to make the user carrier phase positions available again. Instead, the number of epochs elapsed until re-initialization is not of interest, if the mobile object is moving very slowly or the sampling rate is very high. Therefore, to illustrate the advantage of the developed ambiguity resolution procedure, the positions of the seventeenth re-initialization process are presented in the left chart of figure 7. Whilst the single-epoch approach could fix the ambiguities in the second epoch, the commercial software only provided code positions for 277 epochs until the ambiguities could be fixed. During this time, the vehicle covered a distance of almost 400 metres.

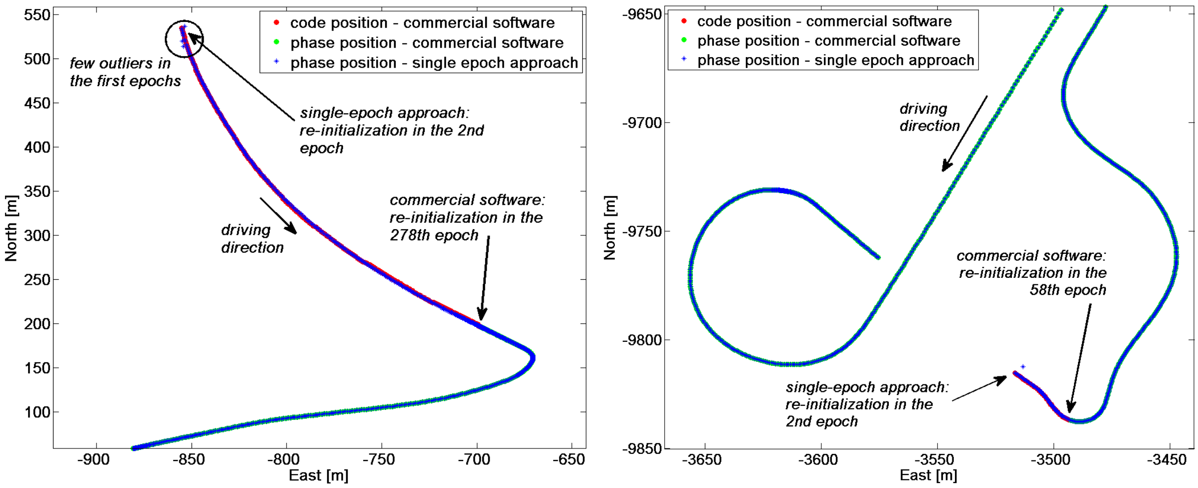

Figure 7: Comparison of results of the single-epoch approach to the outcome of a com. software.

However, it is also conspicuous that there are often few outliers in the first epochs after a signal interruption visible, which are based on poor GNSS conditions due to the proximity to the obstacle, which previously produced the loss of lock. Furthermore, the receiver generally needs different lengths of time to allocate the current carrier-phases. Hence, there are mostly only few observations available in the first epochs after a loss of lock. Certainly, regarding the Kalman filter as well as the variances of the positions, discontinuities become apparent. This is also true for the seventh re-initialization process, which is shown in the right chart of figure 7. In the first epoch after the gap only three poor double differences were available with the result of an incorrect ambiguity resolution. Nevertheless, already one epoch later these ambiguities were fixed correctly, whereas the commercial software required 58 epochs (ca. 32 metres) to provide carrier-phase positions.
Concluding, by combining the approaches to limit the search space with the prediction of the residuals, a fast and reliable procedure to fix the ambiguities could be implemented. Furthermore, the procedure works independently of the application field (low speed in urban areas or high speed on freeways). In most cases only less than 5 epochs are required to find the correct ambiguity resolution, which leads to an ambiguity resolution success rate of 96.59%.

7 CONCLUSIONS

In this contribution we presented an ambiguity resolution approach for kinematic GNSS positioning. Especially in urban areas obstacles lead to frequent losses of lock, which always necessitate a re-initialization of the double-difference ambiguities. Therefore, we developed a single epoch ambiguity resolution to provide carrier-phase positions as fast as possible. In our approach we used the AFM for the determination of the integer number of unknown cycles. To overcome deficiencies caused by the computational efficiency of this procedure we used a combination of an ambiguity resolution in the ambiguity and the coordinate domain for first-time and re-initializations as well as GNSS velocities as long as no interruption occurred, to generate a well-suited search volume. Furthermore, by prediction of the residuals, the unambiguousness of the ARF could be improved. Considering experiments during different applications the approach was tested successfully. Despite frequently poor GNSS conditions an average ambiguity resolution success rate of 96.59% was reached. With few exceptions the integer cycles were re-initialized during the first 10 epochs after every signal interruption, in order that the approach leads to a reliable and fast ambiguity resolution.

REFERENCES

ABIDIN, H.Z.: *On-the-Fly Ambiguity Resolution*, GPS World, April 1994, pp. 40-49, 1994

AUSSEMS, T.: *Positionsschätzung von Landfahrzeugen mittels Kalman-Filterung aus Satelliten- und Koppelnavigationsbeobachtungen*, Veröffentlichung des Geod. Institutes der Rheinisch-Westfälischen Technischen Hochschule Aachen, Nr. 55, 1999

BORGE, T.K., FORSELL, B.: *A new real-time ambiguity resolution strategy based on polynomial identification*, Proc. of KIS'94, Banff, Canada, pp. 233-240, 1994

CHEN, D., LACHAPELLE, G.: *A comparison of the FASF and least-squares search algorithms for on-the-fly ambiguity resolution*, Navigation: Journal of the Institute of Navigation, Vol. 42, No.2, pp. 371-390, 1995

COUNSELMAN, C.C., GOUREVITCH, S.A.: *Miniature interferometer terminals for earth surveying: ambiguity and multipath with Global Positioning System*, IEEE Transactions on Geoscience and Remote Sensing, Vol. GE-19, No. 4, pp. 244-252, 1981

CORBETT, S.J., CROSS, P.A.: *GPS single epoch ambiguity resolution*, Survey Review, Vol. 33, No. 257, 1995

EICHHORN, A.: *Ein Beitrag zur parametrischen Identifikation von dynamischen Strukturmodellen mit Methoden der adaptiven Kalman Filterung*, DGK, Reihe C, Heft 585, München, 2005

FREI, E., BEUTLER, G.: *Rapid static positioning based on the fast ambiguity resolution approach "FARA": theory and first results*, Manuscripta Geodaetica, Vol. 15, No. 4, pp. 325-356, 1990

GREWAL, M.S., WEILL, L.R., ANDREWS, A.P.: *Global Positioning System, Inertial Navigation and Integration*, Second Edition, John Wiley and Sons, 2007

HAN, S., RIZOS, C.: *Improving the efficiency of the ambiguity function algorithm*, Journal of Geodesy (1996) 70, pp 330-341, 1995

HATCH, R.: *Instantaneous ambiguity resolution*, Proc. of KIS'90, Banff, Canada, pp. 299-308, 1990

HOFMANN-WELLENHOF, B., LICHTENEGGER, H., WASLE, E.: *GNSS – Global Navigation Satellite System*, SpringerWienNewYork, Graz, 2008

KIM, D., LANGLEY, R.B.: *A search space optimization technique for improving ambiguity resolution and computational efficiency*, In: Earth, Planets and Space, Vol. 52, No.5, pp. 807-812, 1999

KIM, D., LANGLEY, R.B.: *GPS Ambiguity Resolution and Validation: Methodologies, Trends and Issues*, Proc. of the 7th GNSS Workshop – Intern. Symposium on GPS/GNSS, Seoul, Korea, 2000

LACHAPELLE, G., CANNON, M.E., ERICKSON, C., FALKENBERG, W.: *High Precision C/A Code Technology for Rapid Static DGPS Surveys*, Proc. of the 6th Intern. Geodetic Symposium on Satellite Positioning, Columbus, Ohio, USA, pp 165-173, 1992

MADER, G.L.: *Ambiguity function techniques for GPS phase initialization and kinematic solutions*, Proc. of 2nd Intern. Symposium on precise positioning with the global positioning system, Ottawa, Canada, pp. 1233-1247, 1990

MARTIN-NEIRA, M., TOLEDO, M., PELAEZ, Z.: The *null space method for GPS integer ambiguity resolution*, Proc. of DSNS'95, Bergen, Norway, 1995

REMONDI, B.W.: *Using the Global Positioning System (GPS) phase observable for relative geodesy: modelling, processing and results*, PhD thesis, Center for Space Research, University of Texas, Austin, 1984

SERRANO, L., KIM, D., LANGLEY, R.B., ITANI, K., UENO, M.,: *A GPS Velocity Sensor: How Accurate Can It Be? – A First Look*, Proc. of ION NTM 2004, San Diego, pp. 875-885, 2004

TEUNISSEN, P.J.G.: *Least-squares estimation of the Integer GPS ambiguities*, Invited lecture, Section IV Theory and Methodology, IAG General meeting, Beijing, China, 1993

TEUNISSEN, P.J.G., DE JONG, P.J., TIBERIUS, C.C.J.M.: *The LAMBDA-method for fast GPS surveying*, Proc. of Intern. Symposium 'GPS technology applications', Bucharest, pp. 203-210, 1995

Contact:
Christian Eling,
Institute of Geodesy and Geoinformation, University of Bonn
Nussallee 17, D-53115 Bonn, Germany
phone: +49 (228) 73 3565
fax: +49 (228) 73 2988
Email: eling@igg.uni-bonn.de